.

Citation: *Egypt.Acad.J.Biolog.Sci. (C.Physiology and Molecular biology) Vol. 17(2) pp171-187 (2025)*
DOI: 10.21608/EAJBSC.2025.454211

Egypt. Acad. J. Biolog. Sci., 17(2):171-187 (2025)

Egyptian Academic Journal of Biological Sciences
C. Physiology & Molecular Biology
ISSN 2090-0767
www.eajbsc.journals.ekb.eg

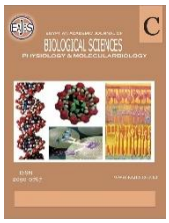

Phytochemical Screening and Evaluation Antibacterial Efficiency of *Artemisia* and *Myrtus communis* Leaf Extracts from the Kurdistan Region, Iraq

Marya M. Othman[1] and Yaseen N. M. ALShekhany[2]

[1]Biology Department, Faculty of Science, Soran University, Soran 44008, Kurdistan Region, Iraq.

[2]Department of Biology, Faculty of Science and Health, Koya University, Koya 44023, Kurdistan Region- F.R., Iraq.

E-mail: marya.othman@soran.edu.iq

ARTICLE INFO

Article History
Received: 14/8/2025
Accepted: 21/9/2025
Available:25/9/2025

Keywords:
Antibacterial chemotypes; Hydroethanolic extracts; Agar-well diffusion; GC–MS; ATR-FTIR; Antimicrobial resistance (AMR);*Artemisia; Myrtus communis*.

ABSTRACT

This study compares the chemical fingerprints and antibacterial activities of 70 % ethanol leaf extracts from *Artemisia* sp. (S1) and *Myrtus communis* (S2) collected in Soran District, Kurdistan region, Iraq. Shade-dried leaves were macerated in 70% (v/v) ethanol (1:15 w/v; 4.00 g in 60.0 mL; 72 h) and profiled by untargeted gas chromatography–mass spectrometry and ATR-FTIR. Antibacterial efficacy was evaluated by agar-well diffusion against *S. aureus*, *E. faecalis*, *E. coli*, and *P. aeruginosa* at 100, 50, and 25 mg mL^{-1} (50 µL per well; final EtOH ≤ 1 % (v/v); n = 3). Extraction yields were comparable (13.01 ± 0.29 % for S1; 13.38 ± 0.22 % for S2). Chemical fingerprints diverged sharply: S2 was rich in a bicyclic monoterpenol plus two imidazole alkaloids (≈ 46 % TIC), whereas S1 contained a sulfur-bearing aziridine and azulene sesquiterpenes. Multivariate analysis associated these chemotypes with preferential antibacterial effects. Bioactivity mirrored composition: S2 produced very large zones against *E. faecalis* (30.7–34.3 mm) and retained Gram-positive potency on dilution, while S1 alone surpassed the 15 mm efficacy benchmark against *P. aeruginosa* (16.7 ± 0.5 mm at 25 mg mL^{-1}). A viscosity-dependent diffusion effect explained S1's inverse dose–response. Given the shrubs' abundance and low cost in Kurdistan, these extracts support Iraq's One Health strategy and merit fractionation, mode-of-action and safety studies.

INTRODUCTION

Antimicrobial resistance (AMR) has shifted from a looming danger to a quantified global disaster: 1.27 million deaths in 2021 were immediately attributable to drug-resistant bacteria, and modeling predictions ~1.9 million direct deaths per year by 2050 if no action is taken (Naghavi *et al.,* 2024). Even though the need for new treatments is pressing, the pharmaceutical pipeline remains shallow. The 2023 WHO antibacterial clinical-pipeline report lists 97 antibacterial agents in clinical development; of the 57 that are traditional small-molecule antibiotics, only 32 target WHO priority pathogens, 12 meet at least one innovation criterion, and just four show activity against a "critical" Gram-negative bacterium (Organization, 2024, Melchiorri *et al.,* 2025). High development expenses—often exceeding US $1 billion and decade-long timelines widen the therapeutic gap (Towse *et al.,* 2017).

Within WHO's Eastern Mediterranean Region (EMR), the 2021 Global Burden of Disease update attributed ≈ 96 000 deaths directly to bacterial AMR (≈ 14 deaths per 100 000) and a further 373 000 deaths to associated drug-resistant infections, emphasizing the urgency of new antimicrobials in the region (Mestrovic *et al.,* 2025).

Traditional medicinal plants thus offer a lower-cost, chemically diverse, chemically various discovery path. Roughly one-quarter of currently licensed small-molecule drugs contain a plant-derived pharmacophore (Newman and Cragg, 2020). High-throughput systems which include gas chromatography–mass spectrometry (GC–MS) and attenuated total-reflectance Fourier-transform infrared spectroscopy (ATR-FTIR) enable rapid, untargeted chemotype profiling. Yet the scope of many modern screens stays narrow, often focusing on one species or one pathogen and seldom linking chemical richness to overall antibacterial performance. Recent examples include GC–MS/FT-IR work on *Alangium salviifolium* that lacked antibacterial testing (Ghosh *et al.,* 2023) and an Iranian survey of 18 herbs that reported antibiofilm activity without accompanying chemical data (Hamidi *et al.,* 2024).

Northern Iraq's Soran District, straddling river valleys (~ 530 m) and Zagros foothills (> 2 300 m), harbours tremendous floristic diversity (Youssef, 2020, Hameed *et al.,* 2016). A 2021–2022 ethnobotanical survey recorded 97 medicinal taxa, with leaves cited above all other organs (44 % of preparations) (Abdulwahid *et al.,* 2023). Among the most frequently mentioned remedies were *Artemisia* sp. leaves domestically derman, traditionally decocted for respiratory and digestive complaints and *Myrtus communis* leaves (murt), used as antiseptic poultices for wounds or brewed for urinary infections (Ahmed, 2016, Ghasemi Pirbalouti *et al.,* 2013, Chalechale *et al.,* 2013).

Beyond clinical care, One Health–relevant risks are evident in local food chains: vancomycin-resistant *Staphylococcus aureus* has been detected in dairy products in the Kurdistan Region, Iraq, indicating potential farm-to-table exposure (Khudher *et al.,* 2023). Practical non-antibiotic measures are already being explored, such as probiotic-fortified beverages (Hameed *et al.,* 2023). Regionally, aquaculture-linked zoonoses underscore the need for low-cost, locally sourced interventions, and plant-derived bioactives have improved fish health and disease resistance(Al Sulivany *et al.,* 2024, Adineh *et al.,* 2024).

Iraq's AMR National Action Plan (2018–2022; update 2026–2030) adopts a One Health approach across the human animal environment sectors (Republic of Iraq. Ministry of Health and Environment, 2018, World Health Organization Regional Office for the Eastern Mediterranean, 2025). Aligned with the WHO Global Action Plan surveillance and laboratory capacity, stewardship/IPC, research and innovation, and awareness (World Health Organization, 2015, World Health Organization. Regional Office for the Eastern Mediterranean, 2022) this study advances research/innovation and supports stewardship by proposing plant-derived, non-antibiotic options to reduce antibiotic pressure in clinical and food-chain settings (Qurbani *et al.,* 2024)

To date, no peer-reviewed study has directly compared *Artemisia* and *Myrtus communis* leaf extracts under identical antibacterial activity tests, leaving their relative chemotype–activity relationships uncharacterized. Because Iraq's National Action Plan on AMR prioritizes low-cost "One-Health" interventions, locally abundant botanicals represent a strategic opportunity. We hypothesised that the contrasting chemotypes of *Artemisia* and *M. communis* could translate into complementary antibacterial spectra.

The present work responds to this gap by coupling untargeted GC–MS and ATR-FTIR fingerprints with dose-tiered agar-well diffusion assays against four WHO-priority bacteria (*S. aureus*, *E. faecalis* , *E. coli* , and

P. aeruginosa) From an initial panel of sixteen Kurdish botanicals we shortlisted two leaf extracts for in-depth analysis: S1, an *Artemisia* sp. loaded with sesquiterpenes and sulfur-bearing aziridines, and S2, *M. communis* enriched in imidazole alkaloids and bicyclic terpenoids. Our objectives are threefold: (i) to generate comprehensive GC–MS and FTIR fingerprints for each extract, (ii) to quantify their in-vitro antibacterial potency at three concentration levels (100 %, 50 % and 25 % stock = 100 mg mL^{-1} (w/v)), and (iii) to investigate chemotype activity relationships via multivariate statistical analysis, identifying functional groups likely responsible for the divergent "Gram-negative-leaning" versus "Gram-positive-focused" phenotypes. By integrating chemistry and bioassay data, we aim to translate Kurdish ethnomedicine into mechanistically informed, policy-aligned antibacterial leads suitable for downstream fractionation, mode-of-action studies, and preliminary safety evaluation.

MATERIALS AND METHODS

Plant Material Collection and Authentication:

Leaves of *Artemisia sp*. (voucher SU-AMR-007) and *Myrtus communis L*. (voucher SU-AMR-016) were harvested in Oct–Nov 2024 from two ethnobotanically significant sites in the Kurdistan Region, Iraq: Delzian (36.71 °N, 44.91 °E; ≈ 1 300 m a.s.l.) and Rawanduz (36.61 °N, 44.52 °E; ≈ 1 700 m a.s.l.). Harvest timing matched local practice to maximize bioactive content(Abdulwahid *et al.,* 2023). Specimens were authenticated by the Botany Section, Faculty of Science, Soran University, and deposited in the Soran University Herbarium for future reference (Rabeler *et al.,* 2019).

Sample Cleaning, Drying and Pulverization:

Fresh leaves were rinsed under tap water, briefly dipped in distilled water, blot-dried, and shade-dried at 25 ± 2 °C, RH < 50 % for 15–20 days until constant weight (Thamkaew *et al.,* 2021). Dried tissue was ground (<60 mesh, stainless-steel mill), passed through a sieve, and stored at –20 °C in amber polypropylene tubes (Azwanida, 2015).

Extraction and Yield Determination:

For each species, 4.00 g of powdered leaf material was macerated in 60.0 mL of 70% (v/v) ethanol (1:15 w/v) at 22 ± 1 °C for 72 h with stirring for 15 min every hour, a protocol shown to optimize phenolic and flavonoid recovery from leafy matrices (Azmir *et al.,* 2013). After filtration through Whatman No. 1 paper, the combined filtrates were concentrated under reduced pressure in a ventilated oven at 29 °C to constant mass, minimizing loss of heat-labile constituents. Extraction yield was calculated as:

$$yield\ (\%) = \frac{\text{dry} - \text{extract mass}}{dry - powder\ mass} \times 100$$

The dried residues were re-dissolved in absolute ethanol to 100 mg mL^{-1}, sterile filtered (0.22 µm), and stored at 4 °C. Each extraction used for yield determination was performed in biological duplicate (n = 2), and yields are reported descriptively as mean ± SD because n is under-powered for inference. For downstream fingerprinting (GC–MS/FTIR) we prepared three independent biological extracts (n = 3); the third batch was dedicated to profiling only and was not weighed for yield**.**

Phytochemical Characterization:

A dual analytical approach was employed to capture both global functional-group profiles and detailed volatile/semi-volatile metabolisms.

Gas Chromatography Mass Spectrometry (GC–MS):

Samples (non-derivatised) were analysed on a Shimadzu Nexis GC-2030 coupled to a GCMS-QP2020 NX with an AOC-20i Plus autosampler. Separation used a DB-5 MS UI column (30 m × 0.25 mm, 0.25 µm). Oven: 40 °C (3 min) → 10 °C min^{-1} → 280 °C (5 min). Helium (99.999 %) at 1.0 mL min^{-1} (constant flow). Injections were splitless for 1.0 min then 1:20 split; injector 250 °C; EI 70 eV; ion source 230 °C; transfer line 280 °C; scan rate ~10 Hz over m/z 40–

550 with a 3.0 min solvent delay. Retention indices (RI) were measured under the same program using an n-alkane C_7–C_{40} ladder (Van Den Dool and Kratz, 1963). Putative identifications required (i) NIST-20 library match ≥ 80 % and (ii) $|\Delta RI| \leq 10$ RI units on DB-5 (≤ 20 where literature variability warranted) against compiled references (Adams, 2017); annotations are reported as MSI Level 2 (Sumner *et al.,* 2007). Common siloxane/tubing artefacts were excluded from biological interpretation. Each biological extract (n = 3 independent preparations) was injected in technical triplicate (intra-day peak-area RSD < 3 %). The complete GC–MS peak list is available from the corresponding author upon request.

ATR–FTIR (Functional- Group Fingerprints):

Spectra were recorded on a Shimadzu FT-IR spectrometer equipped with a diamond ATR accessory. Approximately 2 mg of each dried powder was scanned in triplicate over 4000–400 cm^{-1} (4 cm^{-1} resolution; 32 scans) (Coates, 2000, Wongsa *et al.,* 2022). Background air spectra were collected before each batch. Raw spectra were rubber-band baseline-corrected and vector-normalised in OriginPro, Version 2024b (OriginLab Corporation, 2024);major bands were assigned using standard FT-IR libraries. Contact pressure was maintained at 80 N, and instrument performance was verified before each run with a polystyrene standard.

Antibacterial Potential Analysis using Agar-well Diffusion Technique:

Antibacterial activity was determined by the agar-well diffusion method (Balouiri *et al.,* 2016, Valgas *et al.,* 2007) and interpreted according to CLSI M100, 31st ed. (Humphries *et al.,* 2021). Overnight cultures of *S. aureus* ATCC 25923, *E. coli* ATCC 25922, *E. faecalis* ATCC 29212 and *P. aeruginosa* ATCC 27853 were adjusted to 0.5 McFarland (~1×10^8 CFU mL^{-1}) and diluted to 1×10^6 CFU mL^{-1}. Mueller–Hinton agar plates (4 mm depth) were lawn-inoculated, and 6 ± 0.5 mm wells were filled with 50 µL of plant extract at 100, 50, or 25 mg mL^{-1} (dissolved in absolute ethanol; final EtOH ≤ 1 % (v/v)). These concentrations correspond to 5.0, 2.5, and 1.25 mg extract per well, respectively (w/v = mass of dried extract per mL solvent). Solvent-only wells (≤ 1 % (v/v) EtOH) and blank wells (sterile water) served as negative controls. Thirteen 6 mm Oxoid antibiotic discs acted as positive controls: ciprofloxacin 5 µg was included on every plate as a broad-spectrum benchmark, and organism-specific comparators (listed in Table A1) were selected in accordance with CLSI guidelines. Disc inhibition-zone diameters (IZDs) were verified against CLSI QC ranges; any out-of-range values were excluded from statistical analyses.

Plates were incubated for 24 h at 37 °C, and inhibition-zone diameters were read in millimetres as total edge-to-edge clear zones (including the 6 mm well) and recorded as the mean of two perpendicular caliper measurements; results are reported as mean ± SD (n = 3). To contextualize diffusion effects, dynamic viscosity (mPa·s) of the *Artemisia* extract (S1) stock solutions at 100, 50, and 25 mg mL^{-1} was measured at 25 °C with a rotational viscometer in triplicate (n = 3 per concentration); means ± SD are reported and used solely to interpret agar diffusion (Mezger, 2020).

Statistical Analysis:

Extraction yields (n = 2) and inhibition-zone diameters (n = 3) are presented as mean ± SD. One-way ANOVA with Tukey's HSD post-hoc test ($\alpha = 0.05$) was performed in IBM SPSS v29. ATR-FTIR band scores were clustered by Ward's method (Euclidean distance) in Origin 2024.

RESULTS AND DISCUSSION

Extraction Yield of the Two Lead Extracts*:*

Hydroethanolic maceration produced comparable crude-extract yields from the two species (Table 1). *Artemisia sp*. (S1) afforded 13.01 ± 0.29 % w/w, while *Myrtus communis* (S2) afforded 13.38 ± 0.22 % w/w (mean ± SD; n = 2). No formal statistical test was applied because duplicate replicates are insufficient for reliable inference.

Table 1. Crude extract yields (% w/w) from hydroethanolic maceration of *Artemisia* sp. (S1) and *Myrtus communis* (S2) leaves (mean ± SD, n = 2).

Voucher	Species (leaf)	Yield % w/w (mean ± SD)
S1	*Artemisia* sp.	13.01 ± 0.29
S2	*Myrtus communis*	13.38 ± 0.22

GC–MS Metabolite Fingerprints:

Replicate GC–MS analyses of hydroethanolic (100 mg mL^{-1}) leaf extracts of *Artemisia* sp. (S1) and *Myrtus communis* (S2) were highly repeatable (intra-day RSD < 3 %, n = 3), producing the chromatograms shown in Figures 1A-B and summarized in Table 2. For S1, five well-resolved peaks between 9.43 and 11.27 min dominated the trace, together contributing 24.1 % of the integrated total-ion current (TIC) (Fig. 1A; Table 2A). The most intense signal appeared at 9.97 min (7.81 % TIC) and corresponded to a sulfur-bearing aziridine; four secondary peaks ranged from 6.49 % down to 3.13 % TIC. For S2, the profile was skewed towards a single bicyclic monoterpenol at 8.03 min that alone contributed 28.59 % TIC; four additional signals lifted the top-five share to 52.2 % TIC (Fig. 1B; Table 2B). Sixty-four peaks in S1 and fifty-seven in S2 exceeded the 0.1 % TIC threshold; only those ≥ 1 % are discussed here and reported in Table 2. Tentative identifications were supported by NIST-20 library matches (top-five SI range 65–90) and retention-index agreement ($|\Delta RI| \leq 10$ RI units; ≤ 20 where literature warranted) (Van Den Dool and Kratz, 1963, Adams, 2017, Stein *et al.,* 2014). Outside the top five, no other individual ion exceeded 5 % TIC in either chromatogram, consistent with essential-oil reporting conventions (Adams, 2017). Compound identifications are tentative (MSI Level 2).

A side-by-side bar plot (Fig. 1C) highlights this contrast: the bicyclic alcohol apex in S2 is ≈ 3.7-fold more abundant than the aziridine apex in S1, whereas azulene and thiolated aziridine signals are unique to S1. These compositional differences foreshadow the complementary Gram-positive versus Gram-negative antibacterial spectra discussed under Antibacterial activity and elaborated in the Discussion.

Table 2. Most abundant volatile constituents (top-five peaks) detected by GC–MS in hydro-ethanolic leaf extracts of *Artemisia sp*. (S1) and *Myrtus communis* (S2).

A: *Artemisia* sp. (S1)

Retention time (min)	Compound (tentative)	Area (%)	Molecular formula	Class	Similarity Indices
9.97	1-[N-Aziridyl]propane-2-thiol	7.81	$C_6H_{11}NS$	Thiol / aziridine	69
11.27	Isoaromadendrene epoxide	6.49	$C_{15}H_{24}O$	Sesquiterpenoid epoxide	79
9.70	2-Octanol, 8,8-dimethoxy-2,6-dimethyl-	3.44	$C_{12}H_{26}O_3$	Oxygenated monoterpenoid	66
9.48	Chamazulene	3.23	$C_{14}H_{16}$	Azulene sesquiterpenoid	90
9.43	1-Cyclohexene-1-propanal, 2,6,6-trimethyl-	3.13	$C_{13}H_{22}O$	Monoterpenoid aldehyde	72

B: *Myrtus communis* (S2)

Retention time (min)	Compound (tentative)	Area (%)	Molecular formula	Class	Similarity Indices
8.03	endo-1,5,6,7-Tetramethyl-bicyclo [3.2.0]hept-6-en 3-ol	28.59	$C_{11}H_{18}O$	Bicyclic monoterpenol	71
6.99	1H-Imidazole-4-carboxylic acid, 5-methyl-	12.87	$C_5H_6N_2O_2$	Imidazole derivative	72
5.97	1-Ethyl-2-hydroxymethyl-imidazole	3.90	$C_6H_{10}N_2O$	Imidazole derivative	79
13.56	4-Cyclopentene-1,3-dione,4-(3-methyl-2-butenyl)-	3.46	$C_{10}H_{12}O_2$	Conjugated dione	65
8.74	Bicyclo[2.2.1]heptane-2,3-diol, 1,7,7-trimethyl- (2 exo,3-endo)	3.41	$C_{10}H_{18}O_2$	Bicyclic diol	67

Compounds are listed in descending % TIC. RI_{exp} = experimental Kovats retention index. NIST-20 similarity indices (SI) are reported in the table; identifications are tentative (MSI Level 2). The five peaks listed account for 24.1 % (S1) and 52.2 % (S2) of the TIC; outside the top five, no single component exceeded 5 %TIC.

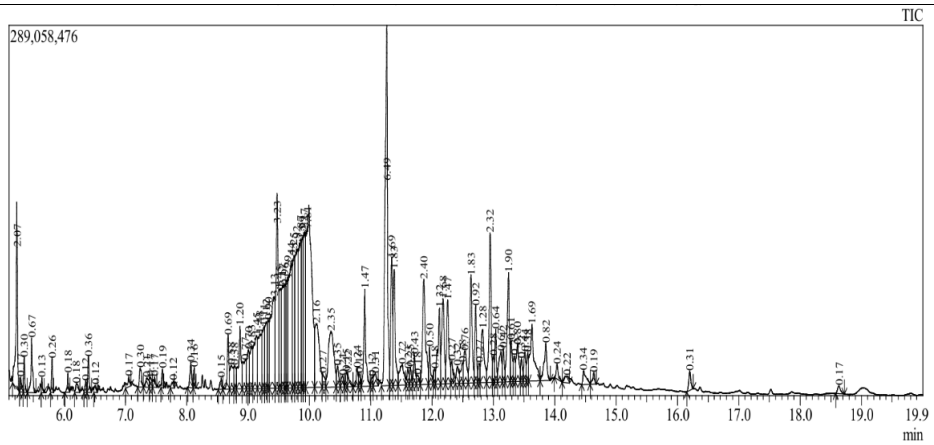

(A) Total-ion chromatogram (TIC) of S1. Five well-resolved peaks at 9.43–11.27 min account for 24.1 % of the integrated ion current; the apex at 9.97 min (7.81 % TIC) is tentatively assigned to 1-[N-aziridyl]propane-2-thiol.

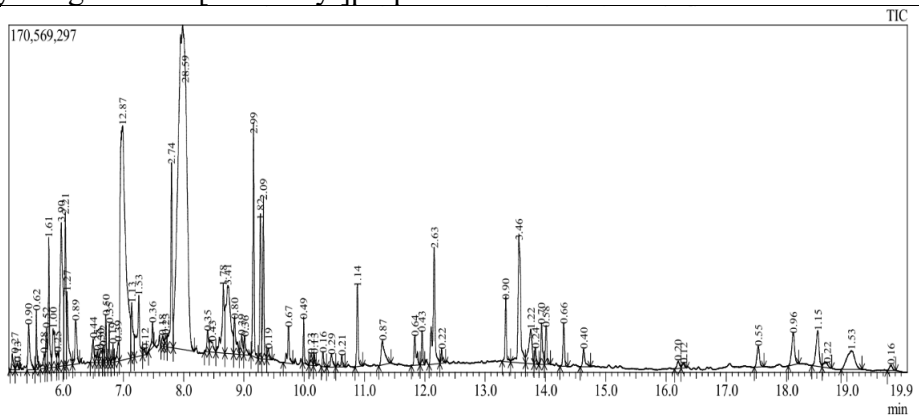

(B) TIC of S2. A single bicyclic monoterpenol at 8.03 min dominates the profile (28.59 % TIC); together with four secondary signals, the top-five peaks contribute 52.2 % TIC.

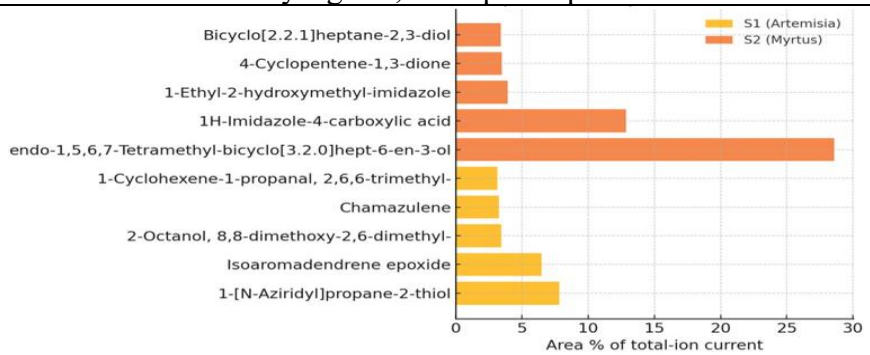

(C) Side-by-side bar plot of the five most abundant constituents in each extract (mean ± SD, n = 3; gold = S1, orange = S2). The bicyclic alcohol in S2 is ≈ 3.7-fold more abundant than the aziridine apex in S1; azulene and thiolated aziridine are unique to S1.

Fig.1. GC–MS fingerprints and chemotypic comparison of hydro-ethanolic leaf extracts from *Artemisia sp*. (S1) and *Myrtus communis* (S2).

ATR-FTIR Functional-Group Analysis:

Replicate ATR-FTIR scans of the hydroethanolic leaf extracts (Figs. 2A–B) were highly consistent (≤1 %RSD on peak intensities, n = 3). Both S1 (*Artemisia sp*.) and S2 (*Myrtus communis*) show the hallmark plant envelope: a broad O–H/N–H stretch centred at ≈3330 cm^{-1} and aliphatic C–H absorptions at 2925/2850 cm^{-1}. Beyond this common core, the spectra diverge. S1 shows

no distinct ester/acid carbonyl at 1735 cm^{-1} (only a faint shoulder), strong aromatic C=C bands at 1610–1500 cm^{-1}, CH_2 bending at 1419 cm^{-1}, and a moderate C–O stretch at 1018 cm^{-1}. By contrast, S2 exhibits a strong carbonyl at 1735 cm^{-1} and markedly stronger O–H and C–O bands at 1230 and 1026 cm^{-1} (Coates, 2000, Smith, 2011). The 1230 cm^{-1} band was assigned to a C–O stretch in phenolic esters, consistent with Smith (Smith, 2011). Table 3 converts six diagnostic bands into a semi-quantitative matrix (✓✓ = strong, ✓ = medium, — = absent). Using Ward linkage on this six-variable dataset (Euclidean distance, no scaling) cleanly partitions the extracts into separate clusters (Fig. 2C), corroborating the chemotypic split inferred from the GC–MS data.

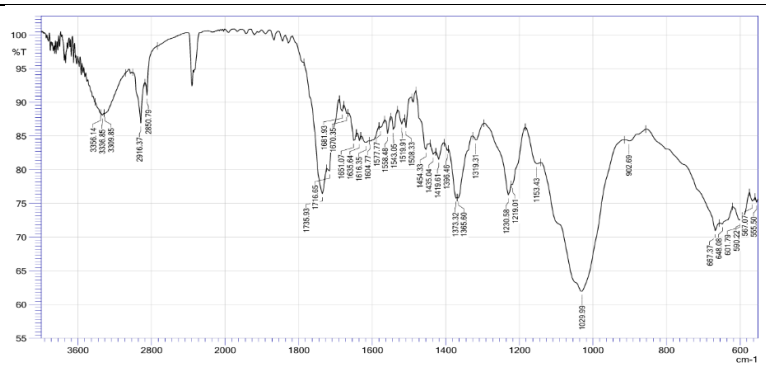

(A) S1: broad O–H/N–H (≈3330 cm^{-1}) and aliphatic C–H (2925/2850 cm^{-1}) envelope; no distinct C=O at 1735 cm^{-1} (faint shoulder only); aromatic C=C (1610–1500 cm^{-1}), CH_2 bend (1419 cm^{-1}), and moderate C–O (1018 cm^{-1}) consistent with sesquiterpenoid/azulene features seen by GC–MS

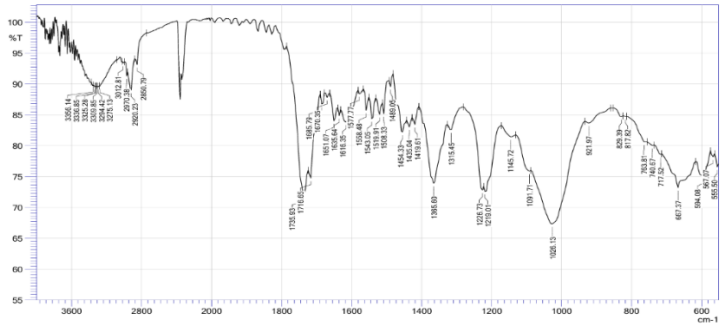

(B) S2: broad O–H/N–H and aliphatic C–H envelope; strong, sharp C=O at 1735 cm^{-1} with intensified C–O at 1230/1026 cm^{-1} consistent with abundant alcohols/esters; weaker aromatic C=C (1610–1500 cm^{-1}) than S1.

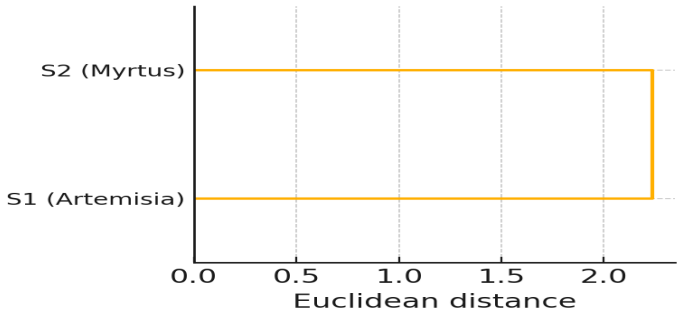

(C) Ward-linkage dendrogram (Euclidean; six bands, Table 3): triplicates cluster tightly (cophenetic < 0.5) and S1 vs. S2 separate at height ~2, indicating that carbonyl and C–O band intensities alone discriminate the two chemotypes.

Fig. 2. ATR-FTIR fingerprints and chemometric comparison of hydroethanolic leaf extracts from *Artemisia sp*. (S1) and *Myrtus communis* (S2).

Table 3. Semi-quantitative ATR-FTIR band matrix for S1 and S2. ✓✓ = *strong;* ✓ = *medium;* — = *absent. Band intensities scored visually from spectra in Figure 2A–B.*

Band (cm^{-1})	3330 (O–H/N–H)	2925 (C–H)	1735 (C=O)	1610–1500 (C=C)	1419 (CH_2)	1018 (C–O)
S1	✓	✓	—	✓	✓	✓
S2	✓✓	✓✓	✓	✓	✓✓	✓✓

Antibacterial Activity:

Inhibition-zone diameters (IZDs; mm, edge-to-edge including the 6 mm well; mean ± SD, n = 3) showed that hydroethanolic extracts (S1, *Artemisia* sp.; S2, *M. communis*) inhibited all four ATCC reference strains (Table 4 & Fig. 3). At 100 mg mL^{-1}, S2 produced IZDs of 30.7 ± 0.6 mm for *E. faecalis*, 17.4 ± 0.6 mm for *S. aureus*, 16.4 ± 0.7 mm for *E. coli*, and 14.1 ± 0.6 mm for *P. aeruginosa*. S1 yielded smaller halos against *E. faecalis* (13.7–19.0 mm) but showed selective activity against *P. aeruginosa*, reaching 16.7 ± 0.5 mm at 25 mg mL^{-1}, satisfying the ≥ 15 mm screening threshold commonly used for agar-well evaluations (Valgas *et al.,* 2007, Balouiri *et al.,* 2016). Across dilutions, IZDs decreased for *E. coli* and both Gram-positive strains with both extracts, whereas *P. aeruginosa* halos increased on dilution with S1 (from 12.1 ± 0.6 mm at 100% to 16.7 ± 0.5 mm at 25%), a pattern consistent with diffusion constraints in agar-based assays (Balouiri *et al.,* 2016, Bonev *et al.,* 2008). One-way ANOVA with Tukey's HSD (α = 0.05) showed S2 > S1 for *E. faecalis* at all doses ($p < 0.05$); for *P. aeruginosa*, S1 > S2 at 50% and 25%, with no difference at 100%; for *E. coli* and *S. aureus* there were no S1–S2 differences. Quality-control disc data are provided in Appendix A, Table A1, and representative plates are shown in Figures A1–A2.

Table 4. Inhibition-zone diameters (IZD, mm) for hydroethanolic leaf extracts of *Artemisia* sp. (S1) and *Myrtus communis* (S2) at three concentrations.

Bacterium	S1 100 %	S1 50 %	S1 25 %	S2 100 %	S2 50 %	S2 25 %
E. coli	16.4 ± 0.7^{a}	12.1 ± 0.6^{a}	11.4 ± 0.7^{a}	16.4 ± 0.7^{a}	12.1 ± 0.6^{a}	11.4 ± 0.7^{a}
E. faecalis	19.0 ± 1.0^{a}	15.3 ± 0.6^{a}	13.7 ± 0.6^{a}	30.7 ± 0.6^{b}	32.3 ± 0.6^{b}	34.3 ± 0.6^{b}
P. aeruginosa	12.1 ± 0.6^{a}	13.7 ± 0.6^{b}	16.7 ± 0.5^{c}	14.0 ± 0.5^{b}	14.6 ± 0.5^{b}	16.8 ± 0.6^{c}
S. aureus	17.4 ± 0.6^{a}	17.2 ± 0.6^{a}	16.6 ± 0.6^{a}	17.4 ± 0.6^{a}	17.2 ± 0.6^{a}	16.6 ± 0.6^{a}

Notes. Values are mean ± SD (n = 3). Mueller–Hinton agar; wells 6 ± 0.5 mm; 50 µL per well; EtOH ≤ 1 % (v/v); 24 h at 37 °C. IZDs measured edge-to-edge (including the 6 mm well). "100/50/25 %" denotes 100/50/25 mg mL^{-1} (w/v), delivering 5.0/2.5/1.25 mg per well. Within each row, values sharing a superscript letter do not differ significantly (one-way ANOVA, Tukey's HSD, α = 0.05

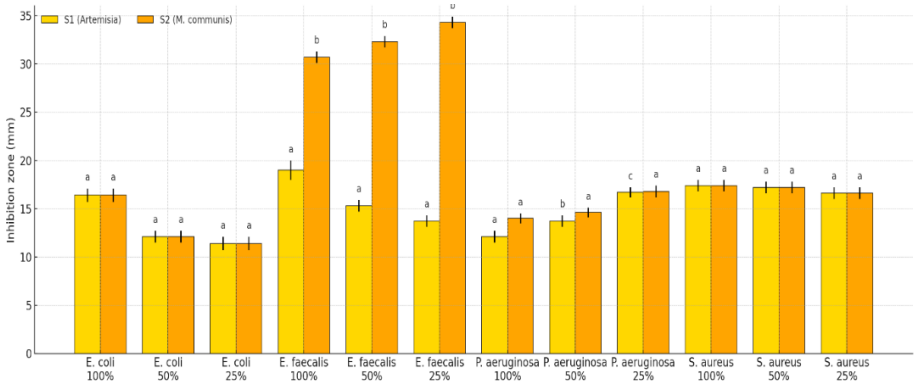

Fig. 3. Inhibition-zone diameters (mean ± SD, n = 3) for hydroethanolic leaf extracts of *Artemisia* (S1, gold) and *Myrtus communis* (S2, orange) against *E. coli*, *E. faecalis*, *P. aeruginosa*, and *S. aureus* at 100 %, 50 %, and 25 % (w/v). IZDs are total edge-to-edge diameters (including the 6 mm well) measured after 24 h at 37 °C on Mueller–Hinton agar; 50 µL/well; EtOH ≤ 1 % (v/v). *E. faecalis* shows the largest zones with S2 (30.7–34.3 mm), while *P. aeruginosa* zones increase as concentration decreases, consistent with diffusion/viscosity effects.

Multivariate Analysis (PCA):

To integrate chemistry with bioactivity, PCA was performed in Origin 2024 with auto-scaling (mean-centred, unit variance) using the five most abundant GC-MS peaks (≥ 1 % TIC) from each extract plus mean IZDs. The first two principal components captured PC1 = 99.8 % and PC2 = 0.2 % of variance. The score plot (Fig. 4A) separated S1 and S2 entirely along PC1. Loadings (Fig. 4B) showed that the bicyclic alcohol (28.6 %) and imidazole alkaloids (12.9 %, 3.9 %) from S2 aligned with strong *E. faecalis* inhibition, whereas the aziridine (7.8 %) and azulenes (6.5 %, 3.2 %) from S1 correlated with selective activity against *P. aeruginosa*. These trends validated the GC–MS, FT-IR and agar-well data, confirming that each chemotype preferentially targeted a distinct bacterial group.

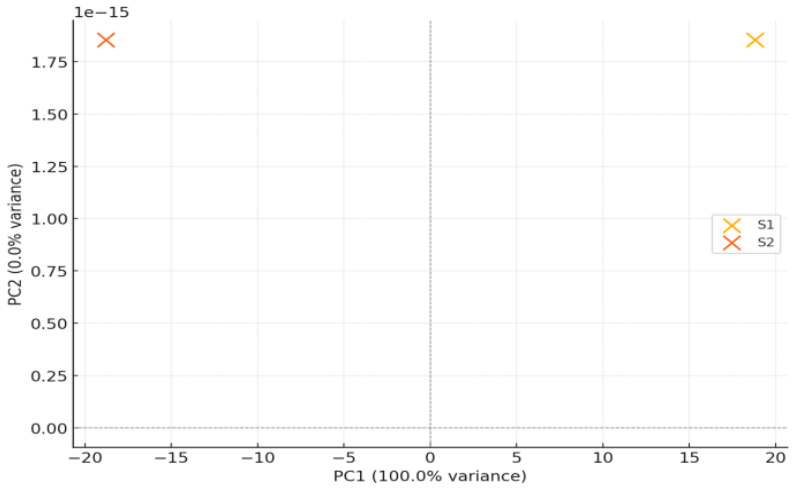

Fig. 4A. PCA score plot (top GC–MS peaks + IZDs): PC1 (99.8% variance) cleanly separates S1 (*Artemisia* sp.) and S2 (*M. communis*). In concert with the loadings (Figure 4B), S2 scores align with the bicyclic alcohol/imidazole features and higher *E. faecalis* inhibition (30–34 mm), whereas S1 scores align with azulene-type sesquiterpenes and selective *P. aeruginosa* activity (16.7 mm at 25 mg mL⁻¹).

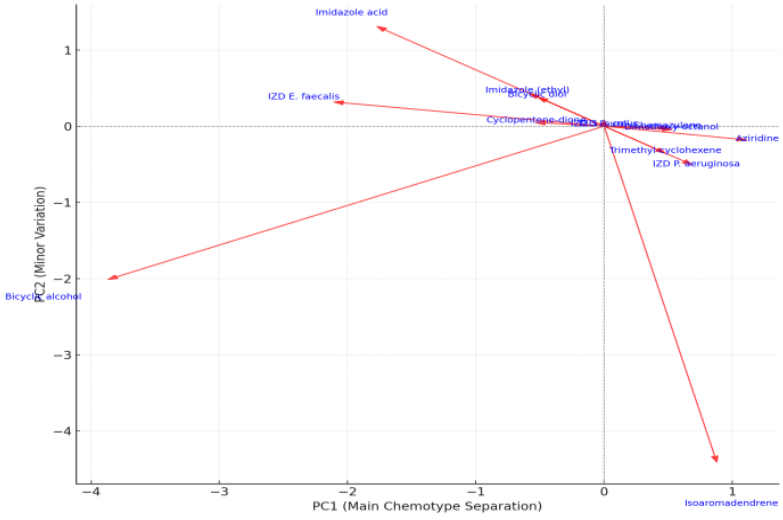

Fig. 4B. PCA Loadings Plot Showing Contributions Of Chemical Peaks And Antibacterial Endpoints To The Separation Of S1 And S2. Arrows Indicate How Variables Load Along PC1 And PC2. Imidazole Alkaloids (12.9%, 3.9%) And Bicyclic Alcohol (28.6%) Drive Gram-Positive Potency (Especially *E. Faecalis),* While Aziridine (7.8%) And Azulenes (6.5%, 3.2%) Drive Gram-Negative Selectivity, Particularly *Pseudomonas Aeruginosa*.

Hydroethanolic maceration yielded *Artemisia* sp. (S1) and *Myrtus communis* (S2) extracts at comparable efficiencies (13.01 ± 0.29 % vs 13.38 ± 0.22 %, n = 2), so the subsequent chemical and antibacterial differences are most parsimoniously attributed to composition rather than process bias. Because duplicate yields are under-powered, we report them descriptively without formal significance testing.

GC–MS indicated that S2 is dominated by a bicyclic monoterpenol (RT 8.03 min, 28.6 % TIC) alongside two imidazole-type features (12.9 % and 3.9 % TIC), whereas S1 contains a sulfur-bearing aziridine (7.8 % TIC), azulene-type sesquiterpenes, and minor oxygenated monoterpenoids. All compound assignments remain tentative (MSI Level 2) as they rely on EI–MS plus measured RI concordance; orthogonal confirmation with authentic standards and/or derivatized GC-MS is planned. Retention indices were measured in this study using a C_7–C_{40} n-alkane ladder under the same program (Van Den Dool and Kratz, 1963) and reconciled against DB-5 compilations (Adams, 2017).

Several headline assignments (e.g., imidazoles, aziridine) are chemically plausible but uncertain without derivatization or authentic standards, so we treat them cautiously pending RI and orthogonal confirmation (Adams, 2017). Mediterranean *M. communis* chemotypes are typically rich in 1,8-cineole, α-pinene, linalool, and myrtenyl acetate, with imidazoles at trace/ND levels (Bekhechi *et al.,* 2019, Bouzabata *et al.,* 2010, Mir *et al.,* 2020, Ben Hsouna *et al.,* 2014). Our S2 appears enriched in a bicyclic monoterpenol and imidazole-type features; rather than claiming a "two-orders-of-magnitude" increase, we frame this as an apparent deviation that requires RI-verified IDs and, given the polarity of imidazoles, derivatized GC-MS for confirmation. The Rawanduz/Delzian collection context (high-altitude, semi-arid calcareous sites) suggests an ecological hypothesis for metabolic shifts that merits seasonal and site-replicated sampling. As summarized in Table 5, comparator leaf oils from Tunisia, Morocco, and Italy are α-pinene/1,8-cineole dominated with imidazoles not detected, underscoring the apparent novelty of the S2 profile (Bakhy *et al.,* 2021, Tuberoso *et al.,* 2006, Dhouibi *et al.,* 2023)

.

Table 5. Reported imidazole alkaloid content in *Myrtus communis* leaf oils

Provenance	Dominant constituents	Imidazole alkaloids (% TIC)
Tunisia (2023)	α-pinene 40%, 1,8-cineole 30%	ND (< 0.1 %) **(Dhouibi et al., 2023)**
Morocco (2021)	Chemotypes: α-pinene/1,8-cineole/linalool; 1,8-cineole/α-pinene; 1,8-cineole/myrtenyl acetate; myrtenyl acetate (multi-site, n = 33)	ND (< 0.1 %)**(Bakhy et al., 2021)**
Italy (2006)	α-pinene ~30.0%, 1,8-cineole ~28.8%	ND (< 0.1 %)**(Tuberoso et al., 2006)**
Kurdistan region, Iraq	bicyclic monoterpenol 28.6%, imidazoles 16.8%	16.8 % **(this study)**

Note. ND = not detected at the method's reporting threshold. The Moroccan entry summarizes chemotypes across seven localities; exact percentages vary by site **(Bakhy et al., 2021)**.

Table 5 shows that Mediterranean leaf oils are typically α-pinene/1,8-cineole dominated with imidazoles not detected, whereas our Northern Iraq sample contains imidazole-type features at 16.8 % TIC.

ATR-FTIR data reinforce the chemotypic split: S2 exhibits a strong carbonyl at 1735 cm^{-1} with intense C–O bands at ~1230/~1026 cm^{-1} (consistent with esters/alcohols), while S1 displays stronger aromatic C=C features (1610–1500 cm^{-1}) compatible with azulenes (Smith, 2011, Coates, 2000). Replicates cluster tightly and the two extracts separate under Ward linkage, indicating analytical reproducibility. These FTIR trends are consistent with the α-pinene/1,8-cineole-dominated literature chemotypes collated in Table 5, while S2

deviates by harboring imidazole-type features.

Both extracts inhibited all four ATCC strains. S2 (*M. communis*) showed pronounced Gram-positive activity, yielding *E. faecalis* zones of 30.7–34.3 mm across 100–25 mg mL^{-1}, whereas S1 (*Artemisia* sp.) was selectively active against *P. aeruginosa*, reaching 16.7 ± 0.5 mm at 25 mg mL^{-1}. Using a ≥ 15 mm screening benchmark for plant extracts, S2 is unequivocally active versus *E. faecalis* and S1 is notably active versus *P. aeruginosa.* One-way ANOVA with Tukey's HSD ($\alpha = 0.05$) confirmed that S2 produced significantly larger inhibition zones than S1 for *E. faecalis* at all doses: no S1–S2 differences were detected for *E. coli* or *S. aureus*. For *P. aeruginosa*, S1 exhibited an inverse concentration–response (12.1 → 13.7 → 16.7 mm from 100 → 50 → 25%), while S2 was comparatively flat (14.0–16.8 mm). Between-extract differences emerged for *P. aeruginosa* at 50% and 25% ($p < 0.05$), whereas 100% did not differ. The S1 trend is consistent with diffusion/viscosity effects in agar-well assays as viscosity decreases (~4.7 → ~1.2 mPa·s) (Balouiri *et al.,* 2016, Bonev *et al.,* 2008). We did not perform MIC/MBC in this study; quantitative potency will be established in future broth MIC/MBC assays (Wiegand *et al.,* 2008). Assays followed the agar-well procedure of Balouiri and Valgas, and antibiotic QC discs were verified against CLSI M100 criteria (Humphries *et al.,* 2021); solvent and blank wells were non-inhibitory. This Gram-positive potency is locally relevant given reports of VRSA in Kurdistan dairy products (Khudher *et al.,* 2023).

S2's ester/alcohol signature and Gram-positive bias are consistent with literature on membrane/permeability effects of oxygenated terpenes in thick peptidoglycan envelopes(Xin *et al.,* 2021, Bakun *et al.,* 2021). S1's azulenes and a sulfurous aziridine map to classes reported to perturb lipid bilayers and, for aziridines, potentially covalently modify cysteine residues (Xin *et al.,* 2021, Bakun *et al.,* 2021, Huang *et al.,* 2022). These are hypotheses requiring validation (e.g., membrane potential/leakage assays, proteomics). Regionally, plant-derived bioactives have improved fish health and disease resistance, supporting the translational potential of such chemotypes (Adineh *et al.,* 2024).

PCA (autoscaled, aligned chemical variables) separated S1 and S2 along PC1 (~99.8 % variance). Because PCA is unsupervised, we treat chemistry–bioactivity associations as exploratory; biplot/loadings suggested that S2's putative bicyclic alcohol/imidazoles align with *E. faecalis* inhibition, whereas S1's aziridine/azulenes align with the *P. aeruginosa* response. Supervised PLS regression is planned to model chemistry→bioactivity links (Jolliffe and Cadima, 2016, Wold *et al.,* 2001).

Given the potential electrophilicity/ genotoxicity of aziridines, Ames mutagenicity and haemolysis/ MTT cytotoxicity are prerequisites to any in-vivo studies (Singh, 2016). Priorities: (i) n-alkane RI measurement and standards for dominant peaks; (ii) future MIC/MBC, time-kill, antibiofilm, and antibiotic-synergy assays in broth; (iii) viscosity/diffusion controls in agar; and (iv) seasonal/site replication to test chemotype stability. Taken together with the comparators in Table 5, the S2 composition suggests a region-specific chemotype that merits seasonal and site-replicated confirmation.From a One-Health AMR perspective, S2 presents a promising Gram-positive lead, while S1 offers a rarer Gram-negative scaffold. These findings align with One-Health priorities across the EMR, where aquaculture-linked zoonoses emphasize affordable interventions (Al Sulivany *et al.,* 2024). Complementary, non-antibiotic strategies such as locally developed probiotic-fortified beverages could be evaluated alongside botanical fractions as co-delivery or sequential approaches (Hameed *et al.,* 2023). Given local availability and low leaf cost, hydroethanolic maceration could be a cost-effective, locally sustainable route to complementary antibacterial leads pending rigorous structural confirmation, safety screening, and future standardized MIC/MBC-based potency testing.

CONCLUSION

Hydroethanolic maceration of two widely used Kurdish botanicals yielded distinct antibacterial chemotypes with complementary effects. The imidazole-rich *M. communis* extract exhibited potent antibacterial activity against *E. faecalis*, producing inhibition zones of up to 34.3 mm, whereas the aziridine/azulene-rich *Artemisia* extract surpassed the 15 mm efficacy benchmark against *P. aeruginosa* even at one-quarter strength. Untargeted spectral profiling revealed that these activities were associated with distinct structural motifs, and agar-well assays confirmed their selective potency. Collectively, these findings identify imidazole-bearing terpenoids and azulene-type sesquiterpenes together with aziridine-containing compounds as promising lead compounds for fractionation, mechanism-of-action studies, and preclinical evaluation within Iraq's One Health antimicrobial-resistance program. By leveraging locally abundant shrubs and a simple hydroethanolic extraction, these leads align with Iraq's One Health AMR priorities—particularly the research-and-innovation pillar—and could support stewardship/IPC by offering low-cost, non-antibiotic options that help reduce antibiotic pressure in human and food-chain settings.

Declarations:

Ethical Approval: This research paper was approved by the research ethics committee from the Faculty of Science, Soran University.

Competing interests: The authors have no competing interests to declare that are relevant to the content of this article.

Authors' Contributions: I hereby verify that all authors mentioned on the title page have made substantial contributions to the conception and design of the study, have thoroughly
reviewed the manuscript, confirm the accuracy and authenticity of the data and its interpretation, and consent to its submission.

Funding: This work has received no external funding.analysis, and manuscript

APPENDIX A

Table A1. Inhibition-zone diameters (mm) of commercial antibiotic discs against ATCC reference strains (mean of three replicates). "—" indicates the antibiotic was not tested against that strain.

Antibiotic (code, 30 µg disc unless noted)	*E. faecalis* ATCC 29212	*E. coli* ATCC 25922	*S. aureus* ATCC 25923	*P. aeruginosa* ATCC 27853
Amoxicillin (AX, 10 µg)	0	13	18	0
Doxycycline (DOX **30 µg)**	15	15	24	10
Tetracycline (TE **30 µg)**	15	13	19	0
Rifampin (RA, 5 µg)	0	0	15	0
Penicillin G (P, 10 U)	0	—	28	—
Oxacillin (OX, 1 µg)	0	—	20	—
Vancomycin (VA, 30 µg)	0	—	18	—
Methicillin (ME, 5 µg)	0	—	0	—
Erythromycin (E **15µg)**	0	—	18	—
Clindamycin (DA **2 µg)**	0	—	24	—
Ciprofloxacin (CIP, 5 µg)	—	35	—	37
Cefepime (FEP, 30 µg)	—	0	—	0
Gentamicin (CN, 10 µg)	—	18	—	23

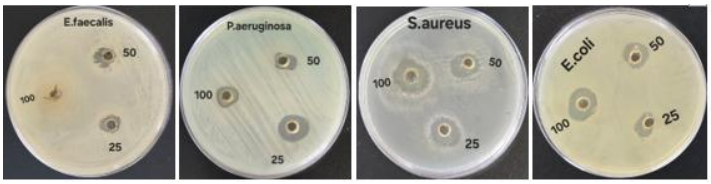

Fig. A1. Representative agar-well diffusion plates showing the dose-dependent activity of the *Artemisia* sp. extract (S1) against the same four bacteria. Note the inverse dose–response against *P. aeruginosa* at 25% concentration.

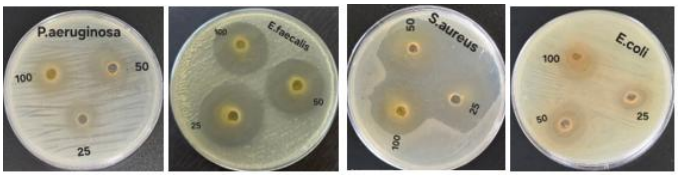

Fig. A2. Representative agar-well diffusion plates showing the dose-dependent activity of the *Myrtus communis* extract (S2) against four WHO-priority bacteria. Wells contain 100%, 50% and 25% (w/v) extract; labels on agar surface correspond to concentration.

REFERENCES

abdulwahid, S., Abdulwahid, M., Magaji, U., Aghwan, Z., Atan, R. & Hamadamin, K. 2023. Medicinal plants used in Soran district Kurdistan region of Iraq, an ethnobotanicals study. *Journal of Pharmacy & Pharmacognosy Research,* 11**,** 1-32.https://doi.org/ 10. 56499/jppres22.1484_11.1.1

Adams, R. P. 2017. *Identification of essential oil components by gas chromatography/mass spectrometry (ed. 4.1)*.978-1-932633-21-4

Adineh, H., Yousefi, M., Al Sulivany, B. S. A., Ahmadifar, E., Farhangi, M. & Hoseini, S. M. 2024. Effects of Dietary Yeast, Saccharomyces cerevisiae, and Costmary, Tanacetum balsamita, Essential Oil on Growth Performance, Digestive Enzymes, Biochemical Parameters, and Disease Resistance in Nile Tilapia, Oreochromis niloticus. *Aquac Nutr,* 2024**,** 1388002.https://doi.org/10. 1155/2024/1388002

Ahmed, H. M. 2016. Ethnopharmacobotanical study on the medicinal plants used by herbalists in Sulaymaniyah Province, Kurdistan, Iraq. *Journal of Ethnobiology and Ethnomedicine,* 12**,** 8.https://doi. org/10.1186/s13002-016-0081-3

Al Sulivany, B. S., Abdulrahman, P., Ahmed, D. Y., Naif, R. O. & Omer, E. A. 2024. Transmission of zoonotic infections (bacteria, parasites, viruses, and fungi) from aquaculture to humans and molecular methods for organism identification. *Journal of Zoonotic Diseases,* 8**,** 580-591.https://doi. org/ 10.22034/jzd.2024.18311

Azmir, J., Zaidul, I. S. M., Rahman, M. M., Sharif, K. M., Mohamed, A., Sahena, F., Jahurul, M. H. A., Ghafoor, K., Norulaini, N. A. & Omar, A. K. 2013. Techniques for extraction of bioactive compounds from plant materials: A review. *Journal of food engineering,* 117**,** 426-436.https://doi.org/10. 1016/ j.jfoodeng.2013.01.014

Azwanida, N. 2015. A review on the extraction methods use in medicinal plants, principle, strength and limitation. *Journal of Medicinal and Aromatic Plants,* 4**,** 2167-0412. https://doi.org/ 10. 4172/ 2167-0412. 1000196ss

Bakhy, K., Belhachmi, T., Benabdelouahab, T., Tomi, F., Casanova, J. & Paoli, M. 2021. Chemical variability of Moroccan myrtle oil. *Chemistry & biodiversity,* 18**,** e2100209. https://doi. org/10.1002/cbdv.202100209

Bakun, P., Czarczynska-Goslinska, B., Goslinski, T. & Lijewski, S. 2021. In vitro and in vivo biological activities of azulene derivatives with potential applications in medicine. *Medicinal chemistry research,* 30**,** 834-846. https://doi.org/10.1007/s00044-021-02726-2

Balouiri, M., Sadiki, M. & Ibnsouda, S. K. 2016. Methods for in vitro evaluating antimicrobial activity: A review. *Journal of Pharmaceutical Analysis,* 6**,** 71-79.https://doi. org/ 10. 1016/j.jpha. 2015.11.005

Bekhechi, C., Watheq Malti, C. E., Boussaïd, M., Achouri, I., Belilet, K., Gibernau, M., Casanova, J. & Tomi, F. 2019. Composition and chemical variability of Myrtus communis leaf oil from

Northwestern Algeria. *Natural Product Communications,* 14**,** 1934578X19850030.https://doi.org/10.1177/1934578X19850030

Ben Hsouna, A., Hamdi, N., Miladi, R. & Abdelkafi, S. 2014. Myrtus communis essential oil: Chemical composition and antimicrobial activities against food spoilage pathogens. *Chemistry & biodiversity,* 11**,** 571-580.https://doi.org/10.1002/cbdv.201300153

Bonev, B., Hooper, J. & Parisot, J. 2008. Principles of assessing bacterial susceptibility to antibiotics using the agar diffusion method. *Journal of antimicrobial chemotherapy,* 61**,** 1295-1301. https://doi. org/ 10. 1093/ jac/dkn086

Bouzabata, A., Boussaha, F., Casanova, J. & Tomi, F. 2010. Composition and chemical variability of leaf oil of Myrtus communis from north-eastern Algeria. *Natural Product Communications,* 5**,** 1934578X1000501029.https://doi.org/10.1177/1934578X1000501029

Chalechale, A., Karimi, I., Zavareh, S. & Karimi, A. 2013. Brief Anthropology and Antiparasitic remedies in Kurdish ethno (Veterinary) Medicine: A neglected treasure trove. *World's Veterinary Journal,* 3**,** 29-32.https://doi.org/10.5455/wvj.20130227

Coates, J. 2000. Interpretation of infrared spectra, a practical approach. *Encyclopedia of analytical chemistry,* 12**,** 10815- 10837. 10. 1002/ 9780470027318.a5606

Dhouibi, I., Flamini, G. & Bouaziz, M. 2023. Comparative Study on the Essential Oils Extracted from Tunisian Rosemary and Myrtle: Chemical Profiles, Quality, and Antimicrobial Activities. *ACS Omega,* 8**,** 6431-6438.http://doi.org/10.1021/acsomega.2c06713

Ghasemi Pirbalouti, A., Momeni, M. & Bahmani, M. 2013. Ethnobotanical study of medicinal plants used by Kurd tribe in Dehloran and Abdanan Districts, Ilam Province, Iran. *African Journal of Traditional, Complementary and Alternative Medicines,* 10**,** 368-85. https://doi.org/10.4314/ajtcam.v10i2.24

Ghosh, S., Sarkar, T. & Chakraborty, R. 2023. Ankol plant (Alangium salvifolium)-The treasure trove of bioactives and medicinal potential. *Food Bioscience,* 51**,** 102230.https://doi.org/10.1016/j.fbio.2022.102230

Hameed, A., Alzubaidy, Z. & Khudher, H. 2023. Preparation of orange juice fortified with probiotics isolated locally from yogurt. *Anbar Journal of Agricultural Sciences,* 21**,** 456-466. https://doi.org/10.32649/ajas.2023.181890

Hameed, M. A., Uzun, A. & Saeed, J. F. 2016. Vascular plant species of Hujran Basin-Erbil/Iraq. *KSÜ Doğa Bilimleri Dergisi,* 19**,** 279-295.https://doi.org/10.18016/KSUJNS.59986

Hamidi, M., Toosi, A. M., Javadi, B., Asili, J., Soheili, V. & Shakeri, A. 2024. In vitro antimicrobial and antibiofilm screening of eighteen Iranian medicinal plants. *BMC Complementary Medicine and Therapies,* 24**,** 135.https://doi.org/10.1186/s12906-024-04437-x

Huang, F., Han, X., Xiao, X. & Zhou, J. 2022. Covalent Warheads Targeting Cysteine Residue: The Promising Approach in Drug Development. *Molecules,* 27.10.3390/ molecules 27227728

Humphries, R., Bobenchik, A. M., Hindler, J. A. & Schuetz, A. N. 2021. Overview of changes to the clinical and laboratory standards institute performance standards for antimicrobial susceptibility testing, M100. *Journal of clinical microbiology,* 59**,** 10.1128/jcm.00213 21.https://doi.org/10.1128/JCM.00213-21

Jolliffe, I. T. & Cadima, J. 2016. Principal component analysis: a review and recent developments. *Philosophical*

transactions of the royal society A: Mathematical, Physical and Engineering Sciences, 374**,** 20150202.https://doi.org/10.1098/rsta.2015.0202

Khudher, H., Alzubaidy, Z. & Abdo, J. 2023. Prevalence of Vancomycin Resistant Staphylococcus Aureus Isolated from Dairy Products in Kurdistan Region-iraq. *The Journal of University of Duhok,* 26**,** 199-206.https://doi.org/10.26682/sjuod.2023.26.2.16

Melchiorri, D., Rocke, T., Alm, R. A., Cameron, A. M. & Gigante, V. 2025. Addressing urgent priorities in antibiotic development: insights from WHO 2023 antibacterial clinical pipeline analyses. *The Lancet Microbe,* 6.https://doi.org/10.1016/j.lanmic.2024.100992

Mestrovic, T., Aguilar, G. R., Swetschinski, M. L. R., Weaver, M. N. D., Wool, M. E. E., Gray, M. A. P., Ikuta, K. S., Han, M. C., Hayoon, M. A. G. & Chung, E. 2025. Insights into the burden of bacterial antimicrobial resistance (AMR) in the WHO Eastern Mediterranean Region: a crucial step towards evidence-informed and targeted public health interventions. *International Journal of Infectious Diseases,* 152**,** 107638.https://doi.org/10.1016/j.ijid.2024.107638

Mezger, T. 2020. *The rheology handbook: for users of rotational and oscillatory rheometers*, European Coatings. 386630532X

Mir, M. A., Bashir, N., Alfaify, A. & Oteef, M. D. Y. 2020. GC-MS analysis of Myrtus communis extract and its antibacterial activity against Gram-positive bacteria. *Journal of BMC complementary medicine and therapies,* 20**,** 86.10.1186/s12906-020-2863-3

Naghavi, M., Vollset, S. E., Ikuta, K. S., Swetschinski, L. R., Gray, A. P., Wool, E. E., Aguilar, G. R., Mestrovic, T., Smith, G. & Han, C. 2024. Global burden of bacterial antimicrobial resistance 1990–2021: a systematic analysis with forecasts to 2050. *The Lancet,* 404**,** 1199-1226.https://doi.org/10.1016/S0140-6736(24)01867-1.

Newman, D. J. & Cragg, G. M. 2020. Natural products as sources of new drugs over the nearly four decades from 01/1981 to 09/2019. *Journal of natural products,* 83**,** 770-803.https://doi.org/10.1021/acs.jnatprod.9b01285

Organization, W. H. 2024. *WHO releases report on state of development of antibacterials* [Online]. Available :https://www.who.int/newsitem/14-06-2024-who-releases-reporton-state-of-development-of antibacterials [Accessed 23 June 2025].https://www.who.int/news/item/14-06-2024-who-releases-report on- state -of-development-of-antibacterials.

Originlab Corporation 2024. OriginPro, Version 2024b. Northampton (MA): OriginLab. https://www.originlab.com

Qurbani, K., Ali, S., Hussein, S. & Hamzah, H. 2024. Antibiotic resistance in Kurdistan, Iraq: A growing concern. *New Microbes New Infect,* 57**,** 101221.https://doi.org/10.1016/j.nmni.2024.101221

Rabeler, R., Svoboda, H., Thiers, B., Prather, L., Macklin, J., Lagomarsino, L., Majure, L. & Ferguson, C. 2019. Herbarium Practices and Ethics, III. *Systematic Botany,* 44**,** 7-13.10. 1600/036364419X697840

Republic Of Iraq. Ministry Of Health And Environment, N. L. R. O. I. M. O. A. 2018. National action plan of antimicrobial resistance in Iraq, 2018–2022. Geneva.

Singh, G. 2016. Synthetic aziridines in medicinal chemistry: a mini-review. *Mini reviews in medicinal chemistry,* 16**,** 892-904.https://doi.org/10.2174/1389557515666150709122244

Smith, B. C. 2011. *Fundamentals of Fourier transform infrared spectroscopy*, CRC press.1420069306

Stein, S., Mirokhin, Y., Tchekhovskoi, D. & Mallard, W. 2014. National Institute of Standards and Technology (NIST) Mass Spectral Search Program for the NIST. *EPA/NIH Mass Spectral Library, National Institute of Standards and Technology Standard Reference Data Program, Gaithersburg,*

Sumner, L. W., Amberg, A., Barrett, D., Beale, M. H., Beger, R., Daykin, C. A., Fan, T. W.-M., Fiehn, O., Goodacre, R. & Griffin, J. L. 2007. Proposed minimum reporting standards for chemical analysis: chemical analysis working group (CAWG) metabolomics standards initiative (MSI). *Metabolomics,* 3**,** 211-221. https://doi.org/10.1007/s11306-007-0082-2

Thamkaew, G., Sjöholm, I. & Galindo, F. G. 2021. A review of drying methods for improving the quality of dried herbs. *Critical Reviews in Food Science and Nutrition,* 61**,** 1763-1786.https://doi.org/10.1080/10408398.2020.1765309

Towse, A., Hoyle, C. K., Goodall, J., Hirsch, M., Mestre-Ferrandiz, J. & Rex, J. H. 2017. Time for a change in how new antibiotics are reimbursed: Development of an insurance framework for funding new antibiotics based on a policy of risk mitigation. *Health Policy,* 121**,** 1025-1030.https://doi.org/10.1016/j.healthpol.2017.07.011

Tuberoso, C. I., Barra, A., Angioni, A., Sarritzu, E. & Pirisi, F. M. 2006. Chemical composition of volatiles in Sardinian myrtle (Myrtus communis L.) alcoholic extracts and essential oils. *Journal of agricultural and food chemistry,* 54**,** 1420-6.https://doi.org/10.1021/jf052425g

Valgas, C., Souza, S. M. D., Smânia, E. F. & Smânia Jr, A. 2007. Screening methods to determine antibacterial activity of natural products. *Brazilian journal of microbiology,* 38**,** 369-380.https://doi.org/10.1590/S1517-83822007000200034

Van Den Dool, H. & Kratz, P. D. 1963. A generalization of the retention index system including linear temperature programmed gas-liquid partition chromatography. *Journal of chromatography,* 11**,** 463.https:// doi.org/10.1016/S0021-9673(01)80947X

Wiegand, I., Hilpert, K. & Hancock, R. E. 2008. Agar and broth dilution methods to determine the minimal inhibitory concentration (MIC) of antimicrobial substances. *Nature protocols,* 3**,** 163-175.https://doi. org/10.1038/nprot.2007.521

Wold, S., Sjöström, M. & Eriksson, L. 2001. PLS-regression: a basic tool of chemometrics. *Chemometrics and intelligent laboratory systems,* 58**,** 109-130.https:// doi. org/ 10. 1016/ S0169-7439(01)00155-1

Wongsa, P., Phatikulrungsun, P. & Prathumthong, S. 2022. FT-IR characteristics, phenolic profiles and inhibitory potential against digestive enzymes of 25 herbal infusions. *Scientific Reports,* 12**,** 6631.https://doi.org/10.1038/s41598-022-10669-z

World Health Organization 2015. Global action plan on antimicrobial resistance. Geneva.

World Health Organization. Regional Office For The Eastern Mediterranean 2022. Advancing the implementation of One Health in the Eastern Mediterranean Region. Cairo.

World Health Organization. Regional Office For The Eastern Mediterranean. 2025. *Iraq moves forward with a new National Action Plan to tackle antimicrobial resistance* [Online]. Available: https://www.emro. who. int/iraq/news/ iraq- moves-forward-with - a-new-national-action-plan-to-tackle-antimicrobial-resistance.html [Accessed 16 August 2025]. https://www.emro.who.int/iraq/news/ iraq-moves -forward- with-a-new-

national- action- plan- to-tackle-antimicrobial-resistance.html.

Xin, H., Hou, B. & Gao, X. 2021. Azulene-based π-functional materials: design, synthesis, and applications. *Accounts of Chemical Research,* 54**,** 1737-1753.https://doi.org/10.1021/acs.accounts.0c00893

Youssef, S. 2020. Endemic plant species of Iraq: from floristic diversity to critical analysis review. *Journal of Duhok University,* 23**,** 90-105.https://doi.org/10.26682/ajuod.2020.23.2.12